Electronic Supporting Information
for

Quasiparticle Energies, Exciton Level Structure and Optical Absorption Spectra of Ultra-narrow ZSiCNRs

Ping Lou
Department of Physics, Anhui University, Hefei 230039, Anhui, China

Table of Contents

FIG. S1: (color online) (a) the longitudinal optical absorption spectra of 2-ZSiCNR including the effect of the electron-hole (e-h) interaction, (b) the transverse optical absorption spectra of 2-ZSiCNR including the effect of the electron-hole (e-h) interaction. Where different Gaussian broadening δ have been used.
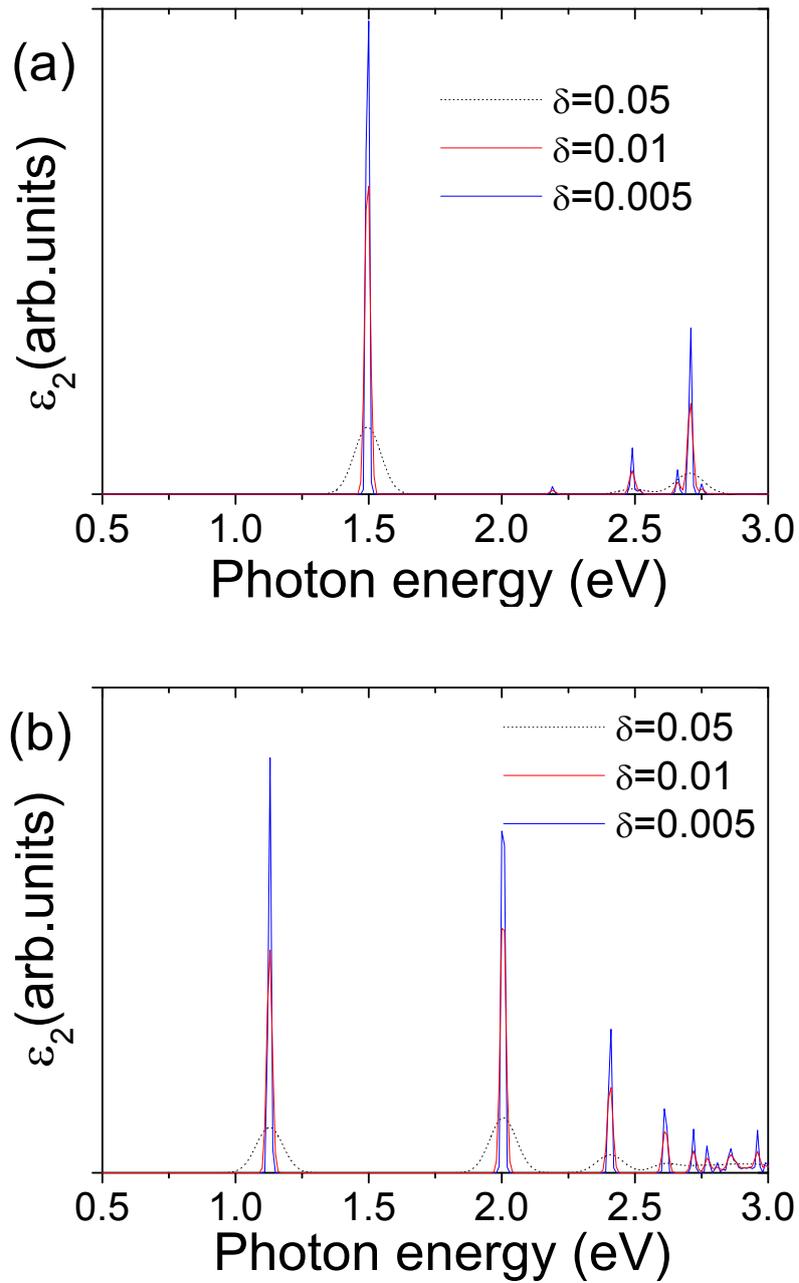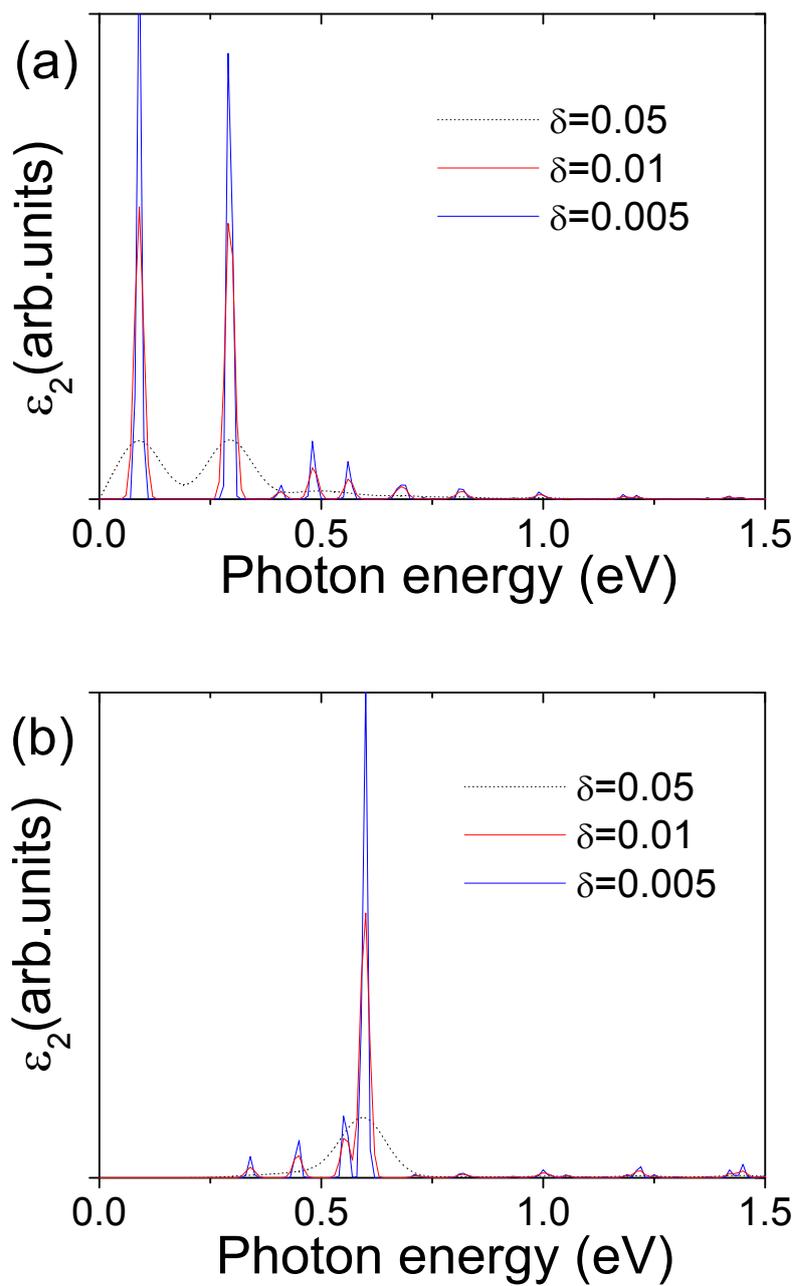
FIG. S2: (color online) (a) the longitudinal optical absorption spectra of 3-ZSiCNR including the effect of the electron-hole (e-h) interaction, (b) the transverse optical absorption spectra of 3-ZSiCNR including the effect of the electron-hole (e-h) interaction. Where different Gaussian broadening δ have been used.

TABLE I: Special analysis for exciton wave functions of the degeneracy energy levels of 2-ZSiCNR associated with the interband transitions E^{ij}.

E^{ij}	n-exciton	Energy (eV)	Weight	Transition point
E^{11}	6	2.489	0.42837	Z
E^{21}	1	2.489	0.53292	Z
E^{11}	10	2.708	0.21162	Z
E^{12}	1	2.708	0.69132	Z

TABLE II: Special analysis for exciton wave functions of the degeneracy energy levels of 3-ZSiCNR associated with the interband transitions E^{ij}.

E^{ij}	n-exciton	Energy (eV)	Weight	Transition point
E^{11}	75	1.814	0.62481	non-Z
E^{21}	1	1.814	0.34912	Z
E^{11}	82	1.936	0.12358	non-Z
E^{21}	2	1.936	0.81733	Z
E^{11}	88	2.054	0.13026	non-Z
E^{21}	3	2.054	0.86282	Z
E^{11}	90	2.107	0.38683	non-Z
E^{21}	4	2.107	0.567292	Z
E^{11}	96	2.176	0.02024	non-Z
E^{21}	5	2.176	0.97640	Z
E^{11}	100	2.220	0.01141	non-Z
E^{21}	6	2.220	0.97691	Z
E^{11}	102	2.258	0.00156	non-Z
E^{21}	7	2.258	0.99704	Z
E^{11}	107	2.312	0.01603	non-Z
E^{21}	8	2.312	0.97002	Z

TABLE III: Convergence of band gap energies E_{g} calculated by GW of N-SiCNRs with respect to the k-grid.

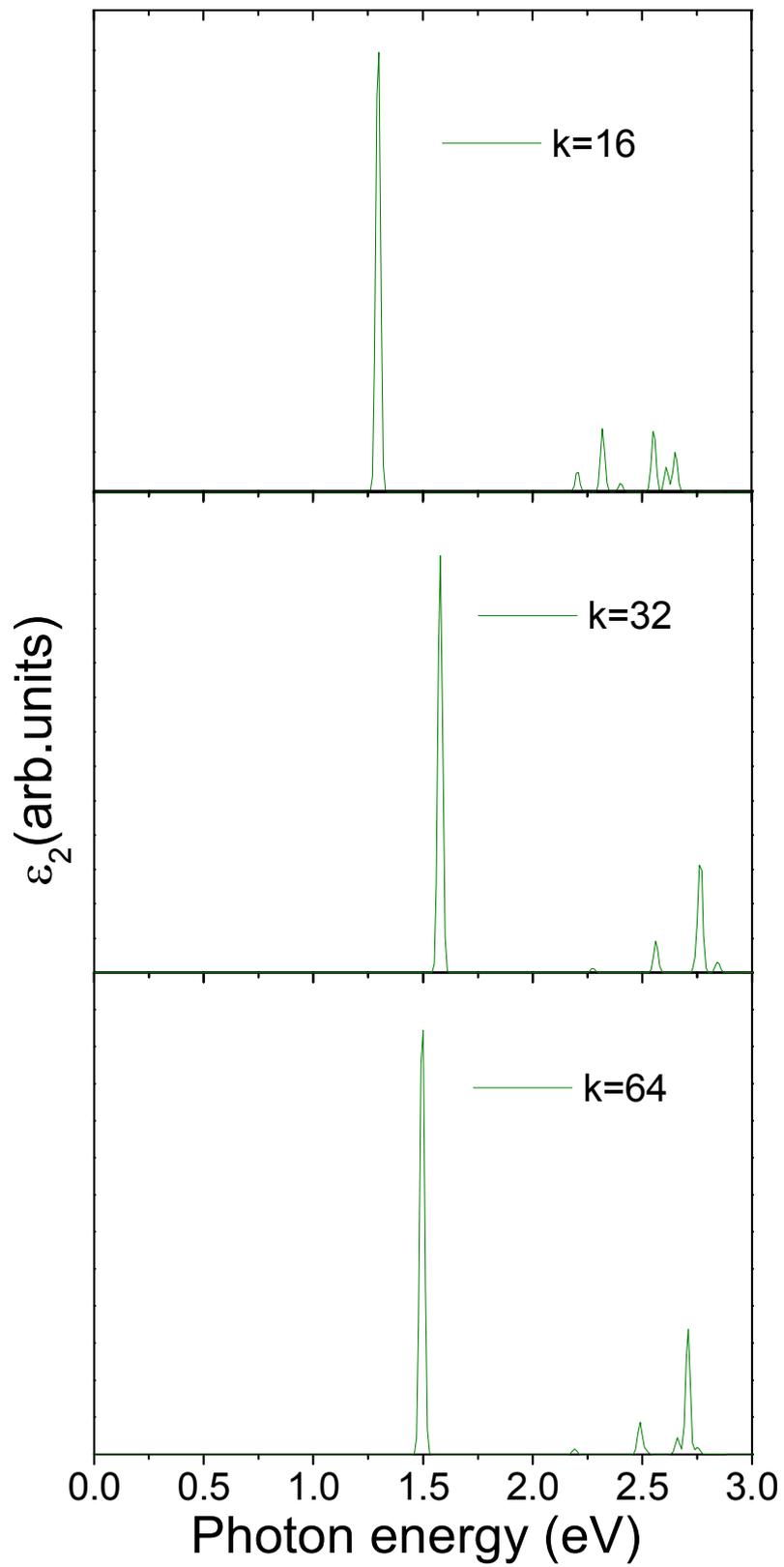| k	2-SiCNR	3-SiCNR
16	2.818 eV	0.949 eV
32	2.909 eV	0.869 eV
64	2.911 eV	0.804 eV

FIG. S3: (color online) Convergence of the optical absorption spectrum with respect to the k-grid. The longitudinal optical absorption spectra of 2-ZSiCNR including the effect of the electron-hole (e-h) interaction. A Gaussian broadening of 0.01 eV has been used.
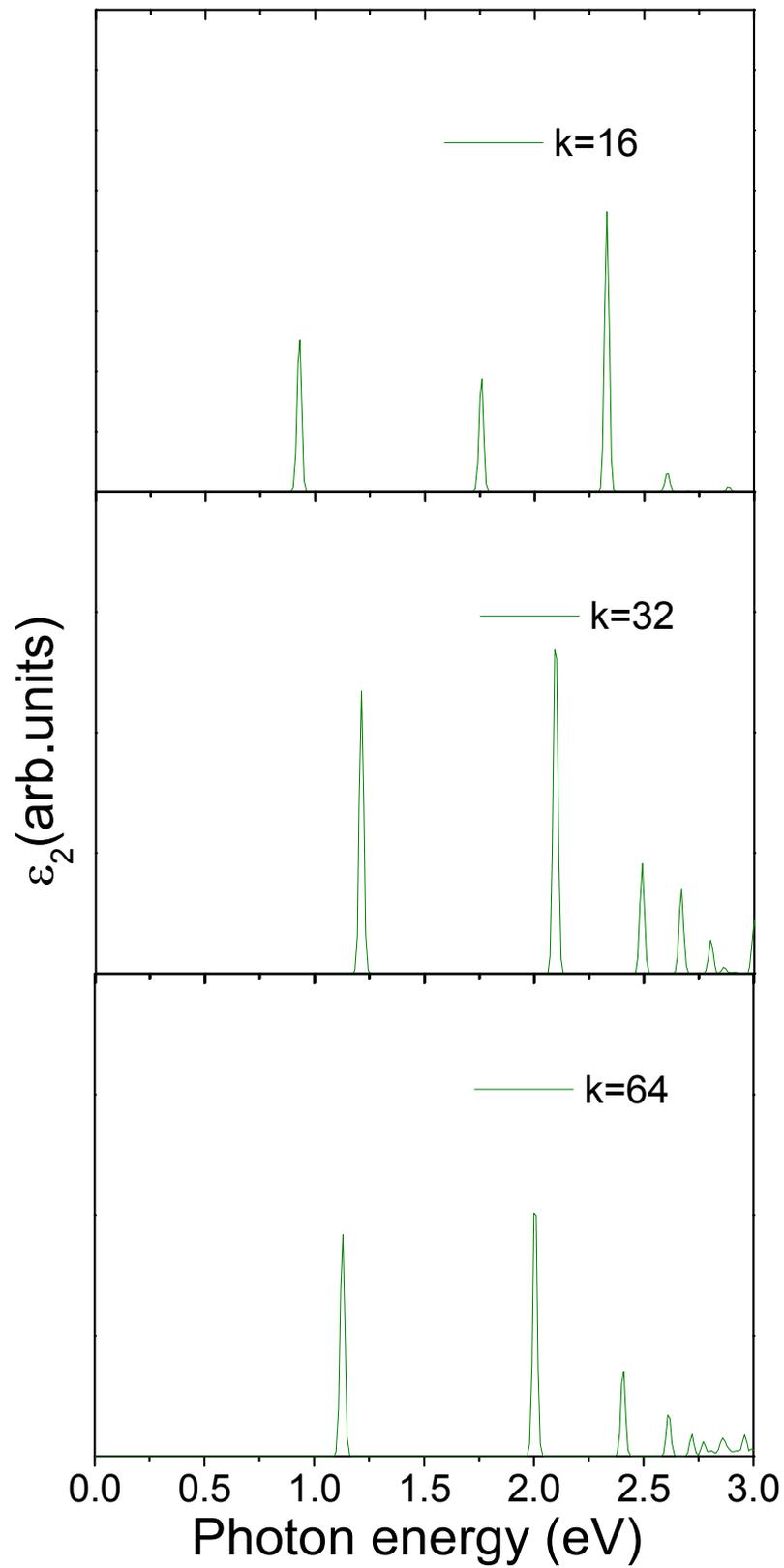
FIG. S4: (color online) Convergence of the optical absorption spectrum with respect to the k-grid. The transverse optical absorption spectra of 2-ZSiCNR including the effect of the electron-hole (e-h) interaction. A Gaussian broadening of 0.01 eV has been used.
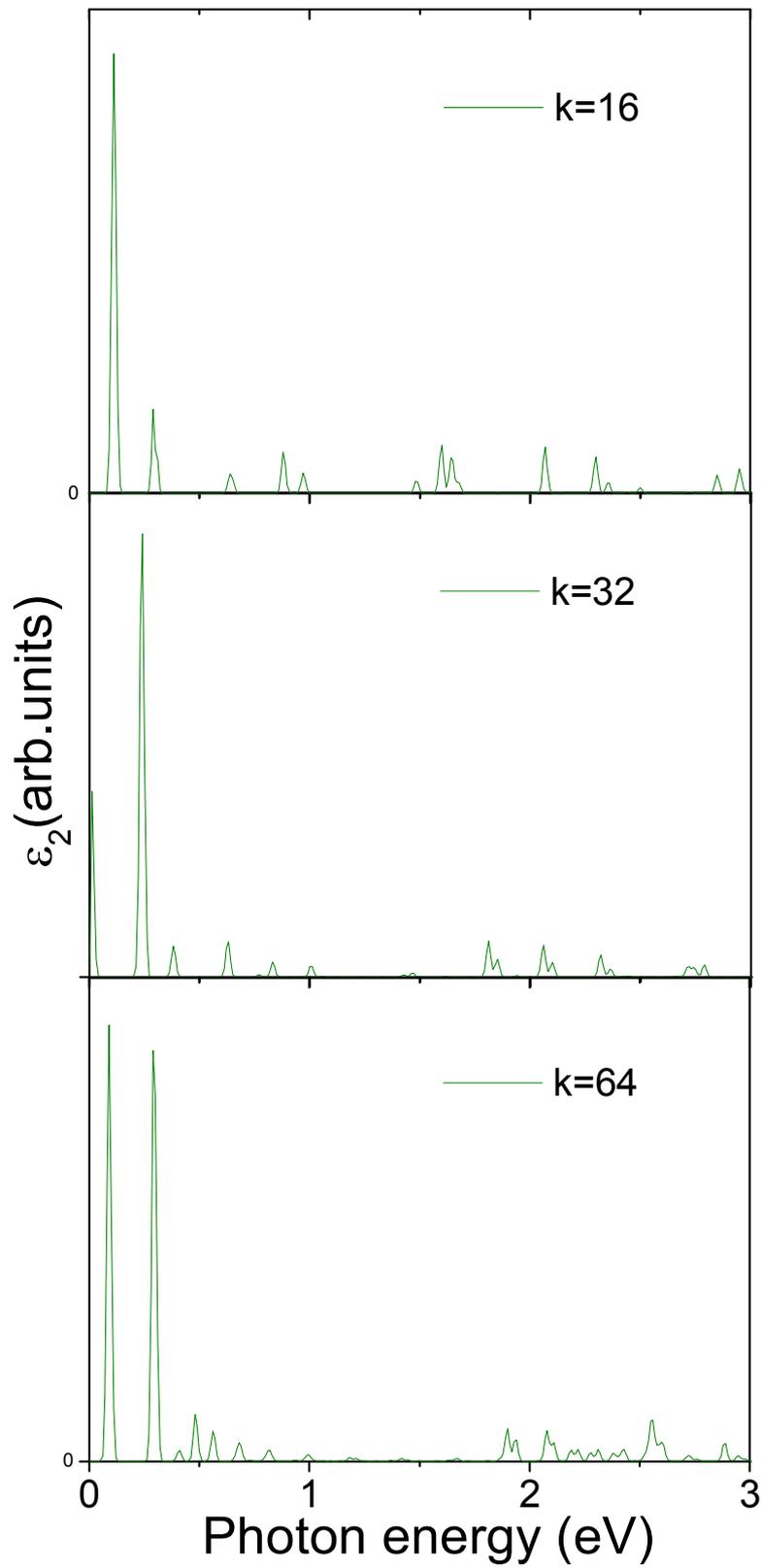
FIG. S5: (color online) Convergence of the optical absorption spectrum with respect to the k-grid. The longitudinal optical absorption spectra of 3-ZSiCNR including the effect of the electron-hole (e-h) interaction. A Gaussian broadening of 0.01 eV has been used.
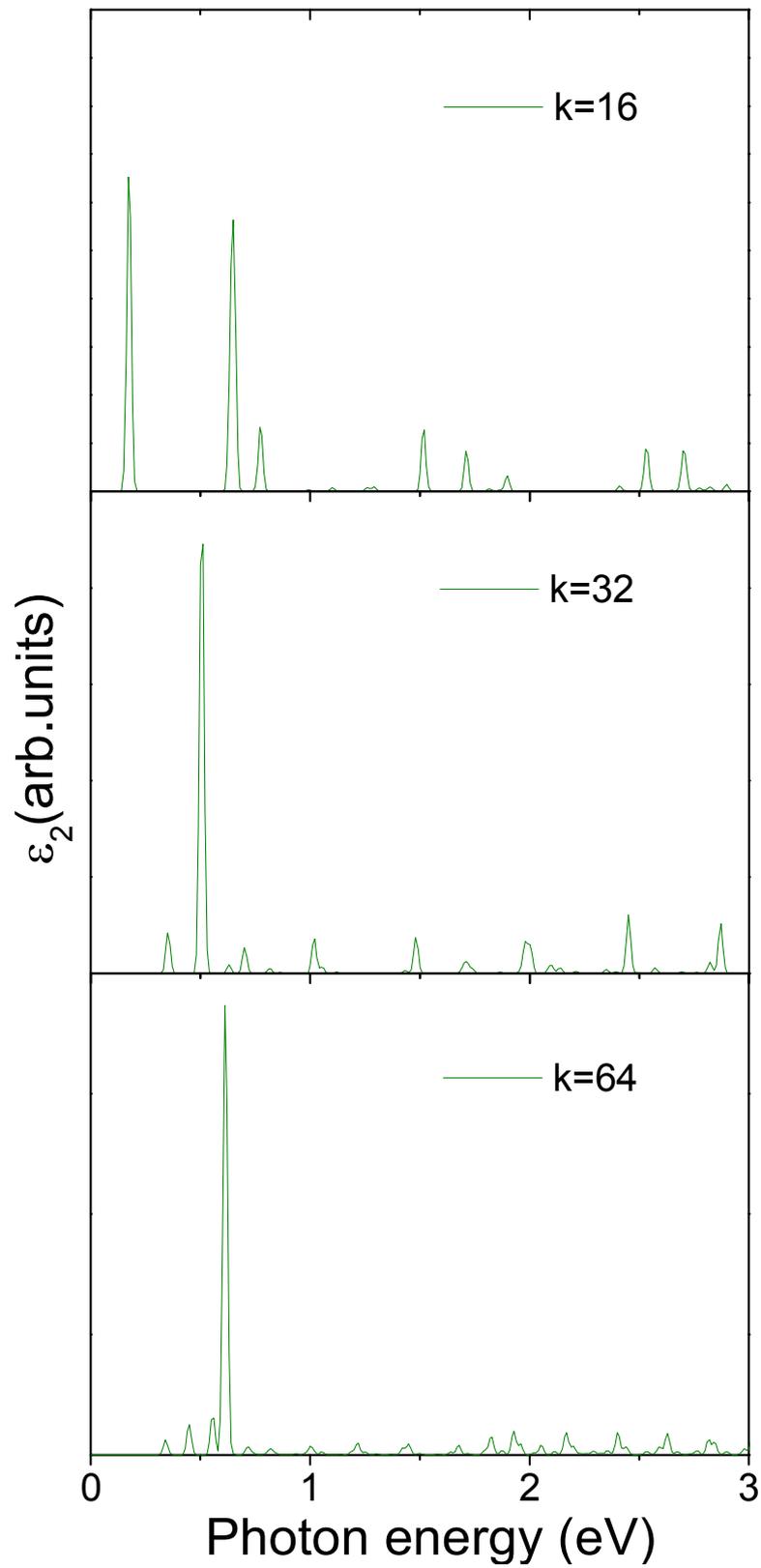
FIG. S6: (color online) Convergence of the optical absorption spectrum with respect to the k-grid. The transverse optical absorption spectra of 3-ZSiCNR including the effect of the electron-hole (e-h) interaction. A Gaussian broadening of 0.01 eV has been used.
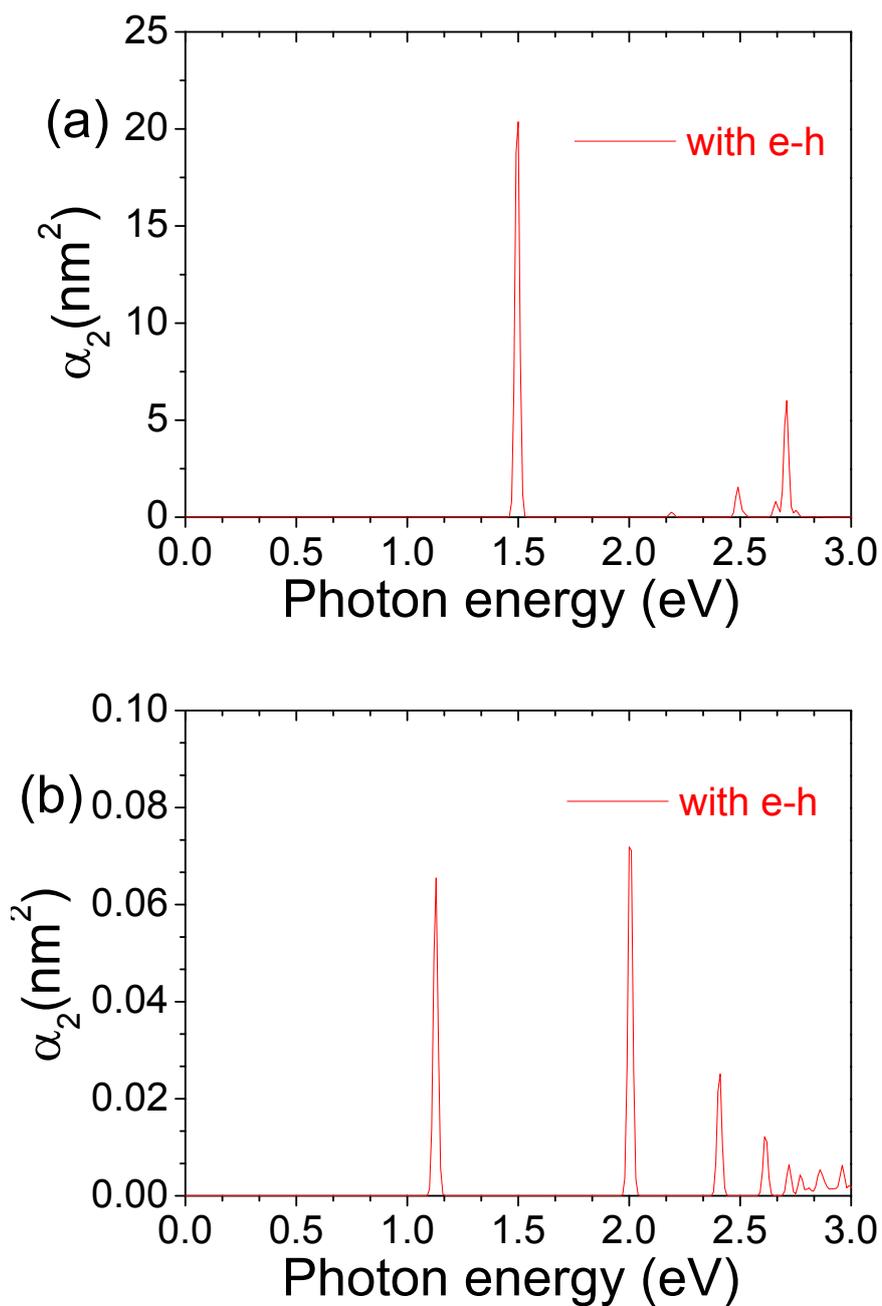
FIG. S7: (color online) The optical spectra in the polarizability per unit area: (a) the longitudinal optical absorption spectra of 2-ZSiCNR including the effect of the electron-hole (e-h) interaction, (b) the transverse optical absorption spectra of 2-ZSiCNR including the effect of the electron-hole (e-h) interaction. Where different Gaussian broadening δ have been used.
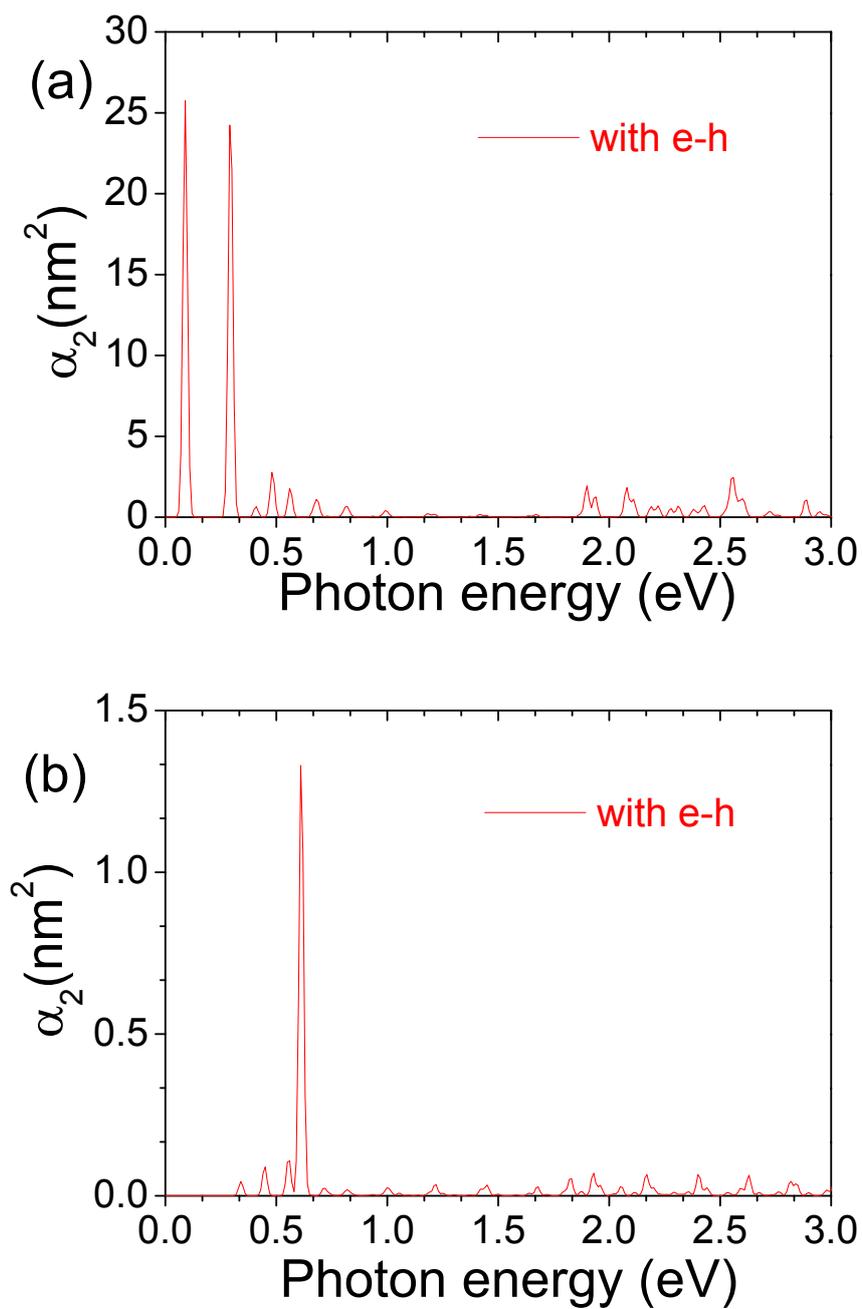
FIG. S8: (color online) The optical spectra in the polarizability per unit area: (a) the longitudinal optical absorption spectra of 3-ZSiCNR including the effect of the electron-hole (e-h) interaction, (b) the transverse optical absorption spectra of 3-ZSiCNR including the effect of the electron-hole (e-h) interaction. A Gaussian broadening of 0.01 eV has been used.